HEFAT2014
10th International Conference on Heat Transfer, Fluid Mechanics and Thermodynamics
14 – 26 July 2014
Orlando, Florida

DUAL-PURPOSE POWER-DESALINATION PLANT AUGMENTED BY THERMAL ENERGY STORAGE SYSTEM

Gude V.G.*, Gadhamshetty V. and Khandan N.N.
*Author for correspondence
Department of Civil and Environmental Engineering,
Mississippi State University,
Mississippi State, MS, 39762,
United States of America
E-mail: gude@cee.msstate.edu

ABSTRACT

This paper presents a novel application of a sensible Thermal Energy Storage (TES) system for simultaneous energy conservation and water desalination in power plants. First, the TES mitigates negative effects of high ambient temperatures on the performance of air cooled condenser (ACC) that cools a 500 MW combined cycle power plant (CCPP); next, the same TES satisfies the cooling requirements in a 0.25 mgd multi-effect distillation (MED) plant. Stack gases from CCPP are used to drive an absorption refrigeration system (ARS) which maintains the chilled water temperature in a TES tank. A process model integrating CCPP, ARS, TES, and MED has been developed to optimize the volume of the TES. Preliminary analysis showed that a tank volume of 2950 m^3 was adequate in meeting the cooling requirements of both ACC and MED in both hot and cold seasons. The proposed TES has the potential to save 2.5% of the power loss in a CCPP/ACC on a hot summer day. Further, our modeling results reveal that a desalination capacity of 0.25-0.43 mgd can be achieved with top brine temperatures between 100 ºC and 70 ºC of MED. The proposed integrated system, process modeling and simultaneous advantages of enhanced CCPP performance and sustainable desalination system will be discussed in the presentation.

INTRODUCTION

Steam power plants reject a major percentage of the input energy as waste heat that is directly discharged to atmosphere. This heat-rejection is accomplished with wet-cooling towers that demand voluminous amount of freshwater. For example, a 500 MW wet-cooled steam power plant consumes ~ 4 million gallons per day of fresh water. The steam-electric plants accounts for nearly 40% of the total freshwater withdrawals in the United States [1]. Dry-cooling technology is an attractive alternative to wet-cooling technology that allows power plants to reject the heat to air, directly or indirectly, without any loss of water [1]. The eminent advantages of dry-cooled power plants include: i) minimal fresh water consumption [2]; ii) flexibility in plant siting that enables power plants to be located closer to load centers rather than to cooling water resources [3]; iii) minimized risk for *Legionella* health risks [4]; and iv) reduced rates of plume formation and brine disposal [5,6]. The major disadvantage of dry-cooling technology is that they use air-cooled condensers (ACCs) whose performance declines with increasing ambient air temperatures, and thereby induces cycle penalties in the associated power plants [7]. The effectiveness of ACCs has been reported to reduce by at least 10% due to high ambient temperatures in summer [1].

The waste heat from the power plants has been found as a suitable source of energy in thermal desalination processes [8, 9]. It is feasible to engineer high-rate desalination systems by incorporating desalination systems in power plants. Such dual-purpose power plants have been reported to deliver substantial cost savings during its entire life-cycle. For instance, the multi-stage flash (MSF) desalination integrated in a steam power plant was able to reduce fuel consumption by 37%; further, such plants were able to reduce water consumption by 45 % compared to a water-only MSF unit [10]. A detailed life-cycle assessment (LCA) study revealed that a dual-purpose power plant reduces environmental impact by 75% compared to a thermal desalination technology [11].

Thermal energy storage (TES) systems offer a viable and feasible approach to store thermal energy when the supply is more than the demand, and to release it when the demand is more than the supply [12]. For example TES systems can be designed to store solar heat energy during sunlight hours of the day and release it for space heating during colder periods of the day, and similarly, for freshwater production in desalination systems powered by waste heat or solar energy [13, 14]. The viability of TES systems has been demonstrated in large-scale applications including heating, ventilating, and air conditioning (HVAC) systems, gas turbines [15-18], district cooling systems [19], and district heating systems [20].

This paper presents a novel application of sensible thermal energy storage (TES) to integrate multi-effect evaporation desalination system (MED) in a combined cycle power plant (CCPP) for simultaneous energy conservation and water desalination. Our objectives in this study are two-fold. First, we will demonstrate that the TES mitigates the negative effects of high ambient temperatures on the performance of air-cooled condenser (ACC); next, we will demonstrate a new method for obtaining 0.25 mgd (950 m^3/d) multi-effect distillation (MED) using waste heat in CCPP and the chilled water from TES.

PROPOSED PROCESS CONFIGURATION

Fig. 1 shows a conceptual schematic of the thermal energy storage (TES) that integrates combined cycle power plant (CCPP) with absorption refrigeration system (ARS) and a multi-effect evaporation desalination system (MED). A TES tank is used to maintain the cooling efficiency of ACCs during hot days, and enables CCPP operation at rated power, instead of suffering power loss due to increased steam turbine backpressure. The waste heat in the CCPP is used to drive an absorption refrigeration system (ARS) that cools chilled water in a TES tank. The chilled water is then used to precool the inlet air to the air-cooled condenser and improve the performance of the CCPP during hot summer. The TES meets the cooling needs of a 0.25 MGD multi-effect desalination (MED) plant. Further, the MED is solely driven by the waste heat available in stack gases. The state points for CCPP, ACC, ARS, TES, and MED are shown in **Fig.2**. The specific technical details for MED are shown in **Fig.3**.

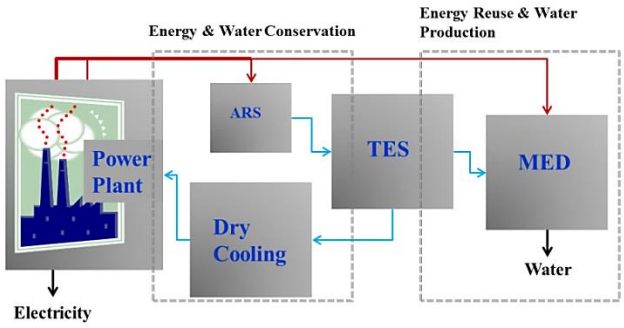

Figure 1. Dual-purpose power-desalination plant supported by thermal energy storage

Combined Cycle Power Plant (CCPP)

The CCPP is comprised of a compressor (COMP), combustion chamber (CC), gas turbine (GT), and heat recovery steam generator (HRSG) (Brayton cycle in **Fig. 2**). The heat discharged from HRSG is used to drive a steam power plant consisting of a steam turbine (ST), open feed heater (OFWH) and the ACC (Rankine Cycle in **Fig. 2**). Atmospheric air is drawn into the compressor (8) and fed to the combustion chamber operating at constant pressure. The high temperature gases enter the gas turbine (10) that producing net-work, W_{GT}. The exhaust gases from the gas turbine (11) are used to produce superheated steam in HRSG (5). The steam turbine produces net-work, $W_{ST.}$ A fraction of the steam turbine exhaust (6) is diverted to the OFWH, where it is mixed with feed water (2)

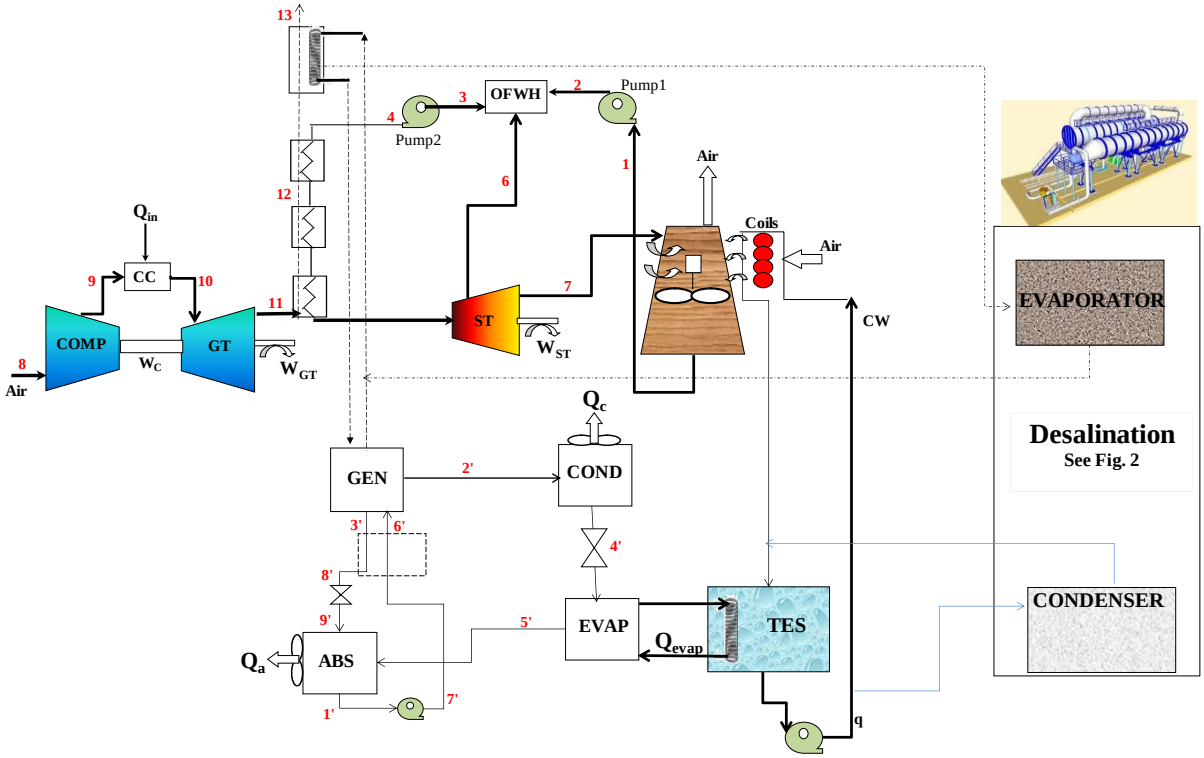

Figure 2. Dual-purpose power-desalination plant supported by thermal energy storage

pumped from the ACC. The remaining fraction of the steam turbine exhaust (7) is returned to the ACC to obtain feed water for reuse (1). Saturated liquid (3) at heater pressure is pumped by pump 2, to HRSG to generate superheated steam (5) to complete the cycle.

Thermal Energy Storage (TES)

The TES is designed to meet the cooling requirements of both the ACC and MED systems. The working fluid in the TES system is water that is maintained at 5ºC by the evaporator of the ARS. We choose water as working fluid as it provides high energy capacity, transfers heat to air at higher efficiency, and offers safety in long-term operations [21]. A chilled water (CW) pump circulates water from the TES through two cooling coils, one installed at the air inlet to the ACC (**Fig.2**), and another, in the final condenser in the MED system (**Fig. 3**). The CW pump supplies cooling water to ACC system only when the ambient temperature exceeds the ACC design air inlet temperature, *T**. The cooling water runs through the final condenser of MED system to remove the latent heat from the vapor generated in the last effect. The flow rate of the chilled water is controlled to maintain inlet air temperature of ACC at the design value of T*, and temperature of CON in MED at T_{cw}. The net external energy in the proposed system are due to the: i) pump in the ARS to transfer the dilute solution from the absorber to the generator, running 24 hours/day; ii) pump to circulate the chilled water from the TES through the cooling coils (running 6 to 8 hours/day); iii) fans for the air-cooled condenser and absorber of the ARS; and iv) pump to circulate the cooling water from the TES to MED final condenser.

Multi-effect evaporation desalination (MED) system

The Multi-effect evaporation desalination (MED) systems are known for high thermal energy efficiency, lower capital costs, and reduced operational costs. The steam in the first effect of MED is supplied by the waste heat extracted from the stack gases (12-13) in CCPP (**Fig. 2**). The heat from condenser of MED is rejected to cooling water stream from the TES (**Fig. 2**). The stack gases in the CCPP are available in the temperature range of 120-150 ºC (Fig. 2), and we therefore considered a MED unit at a top heat source (steam) temperature of 100ºC. The MED operating at higher temperatures (about 100ºC) offer following pre-eminent advantages over MSF [28]: 1) high thermal efficiency with a lower number of effects, 2) high heat transfer coefficient, 3) relatively low specific investment cost, 4) low pumping power, and 5) operating flexibility with short start-up period and 6) demonstrated capability for matching production volume with water demand and energy supply.

The specific number of stages (n) in MED depends on the top brine temperature and the allowable temperature drop between the stages [22]. **Fig. 3** provides the state points for various components in the proposed MED. The heat source in the first effect promotes the evaporation of incoming preheated saline water (feed). The temperature of the vapor in the first effect (T_{v1}) is less than the boiling temperature (T_1) by the magnitude of the boiling point elevation (BPE_1). The vapor in the first effect is transported to the second effect through a demister. The latent heat of condensation (D_1) is exploited for further evaporation in the second effect. The unevaporated brine in the first effect (M_f - D_1) flows through the second effect that operates at a lower pressure. The vapor formed in the second effect can be attributed to the two mechanisms. First, the vapor is generated by boiling the liquid over the heat transfer surfaces D_2. Second mechanism can be attributed to flashing, i.e. free boiling, within the bulk liquid (d_2). The temperature of the vapor due to flashing (Tv_2) differs from the boiling temperature (T_2) by the magnitude of boiling point elevation (BPE_2). Small quantity of vapor (d_2) condenses in the flashing box due to the flashing of distillate condensed in the second effect (D_1). The processes occurring in the second effect are repeated in each subsequent effect all the way down to the last [23].

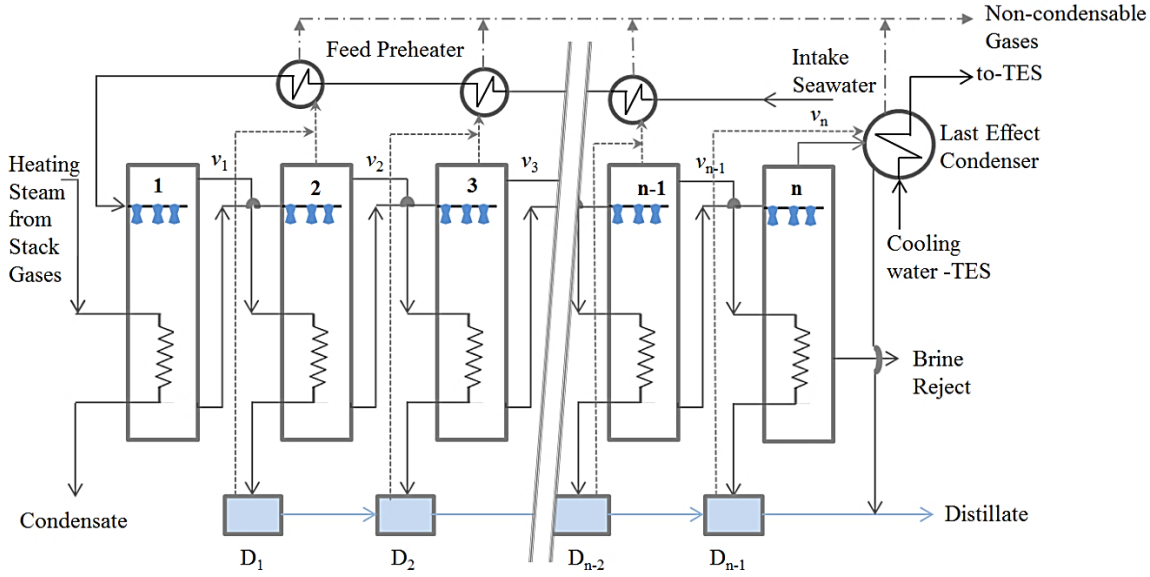

Figure 3. Multi-effect evaporation desalination plant supported by thermal energy storage

RESULTS AND DISCUSSION

The TES tank volume was determined as 2,950 m^3. Simulation results obtained from the model were used to develop performance curves to aid in preliminary evaluations and conceptual designs for ACC and MED.

Ambient Temperature Profiles

The typical ambient temperature for Mccarran Station in Nevada, ranges from -10 to 40 °C, with summer temperatures reaching as high as 39 °C. In general, the high ambient temperature (> T*) reduces the theoretical minimum attainable temperature of air-cooled condensers (in CCPP), and thereby reduces cooling efficiency of ACC, and ultimately incur cycle penalties in a steam turbine of CCPP. From the frequency profiles shown in **Fig. 4**, the performance of the ACC deteriorates for nearly ~50 % of the total operating hours throughout the year, especially, when the ambient air temperature (T_i) is higher than that of air inlet design temperature (T* = 20 °C) (**Fig. 5a**).

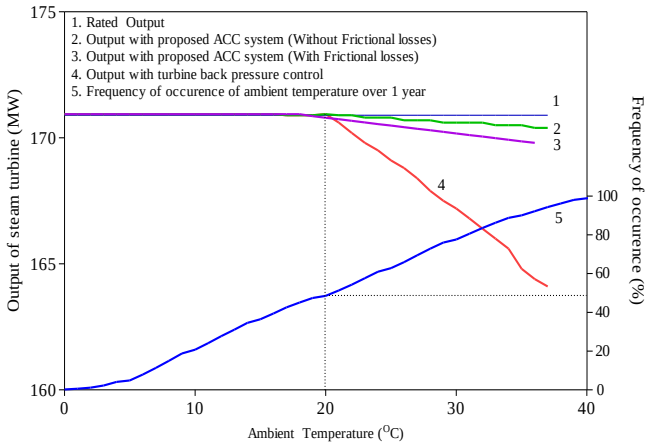

Figure 4. Enhanced performance of CCPP due to ACC modified with TES system

Inlet Air Temperature Profiles of ACC with Proposed TES

The benefit of the TES system in maintaining the steam turbine output at various ambient temperatures is illustrated in **Fig. 4**. As shown in **Fig. 4**, the performance of CCPP decreases with increasing ambient temperatures due to reduced cooling capacity of ACC systems. For instance, the power output of CCPP drops by 4.6 MW at dry bulb temperature of 32 °C, and nearly 10 MW at 35 °C. The cycle penalties in CCPP can be mitigated by maintaining T_i closer to T* on hotter days of the year. **Fig. 5b** shows the temporal profiles of ACC inlet temperature, and **Fig. 5c** depicts the TES tank temperature. The results in **Fig.6** demonstrate the utility of TES system in pre-cooling the ambient air and maintaining its temperature at T*. The most important finding is that the chilled water temperature in TES returns to its original value at end of annual cycle. Therefore, the proposed TES system can be used to maintain cooling requirements in both ACC and MED throughout the year.

Power Penalty imposed by ACCs in CCPP during hotter days

The current practice of turbine back pressure control results in explicit loss of power in the steam power cycle of CCPP due to negative effects of high ambient temperatures on the performance of ACCs. **Fig. 4** demonstrates the utility of TES in improving the cooling efficiency of ACC, and reducing the cycle penalties of CCPP during high ambient temperatures.

Fig. 4 shows the simulated power losses at ambient temperatures ranging from 5 ºC to 40 ºC for the two systems. With increasing ambient temperatures, the loss of power with back pressure control is significantly higher than the loss associated with the proposed system. For example, at a dry-bulb temperature of 32 ºC, the efficiency of cooling is restored to such an extent that the power loss of 4.2 MW is eliminated.

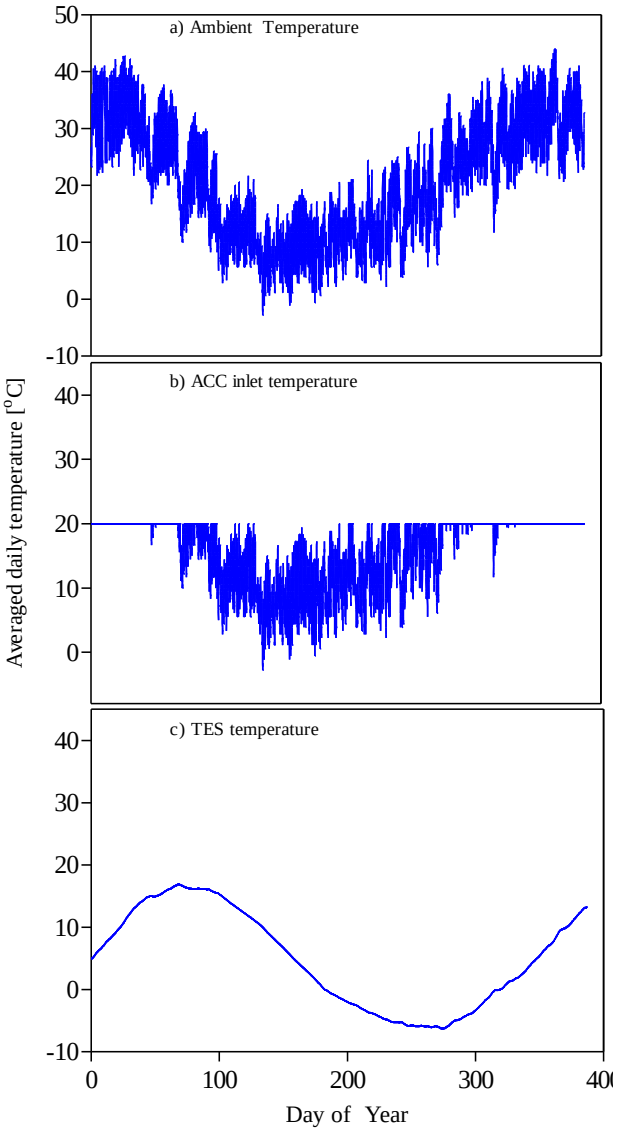

Figure 5. Temperature profile of ambient air, ACC inlet, and TES

The minimum power losses in CCPP with proposed TES/ACC system is due to chilled water pump and the refrigerant transfer pump (Curve 2, **Fig. 4**). In real applications, the energy consumption for pumps (i.e. chilled water pump, refrigerant pump) may be significantly higher due to inherent frictional losses in the fluid systems. Curve 3 in **Fig. 4** shows the effect of frictional losses (assuming ~ 100% of base energy consumption) on the net power output with proposed ACC. It is clear that the proposed ACC can achieve significant power savings in real time applications for typical temperature ranges encountered on a hot summer day (Curve 5, **Fig. 4**).

4.4. Multi-effect Desalination System (MED)

4.4.1. Effect of Heat Source Temperature

Fig. 6a shows the thermal energy requirements of MED as the function of heat-source temperature (70 ºC to 100 ºC) and the number-of-stages (n=6-10). **Fig. 6a** shows that the energy requirements for desalination increases with increasing heat source temperatures. Further, lowest thermal energy requirements are observed at operating conditions imposed by low heat source temperature and highest number of stages (i.e. 70 ºC; n= 10). The energy requirements in MED (~ 2.87-4.85 MW) can be obtained from the stack gases of CCPP (**Fig. 2**). **Fig. 6b** shows the top-brine temperatures as function of heating steam temperatures and the number-of-stages (n = 6-10). The top-brine temperature for 10 stages is 95.5 ºC and 92 ºC for 6 stages. The same are 68.1 ºC and 66.6 ºC for corresponding stages of 10 and 6. The lowest top-brine temperature value corresponds to 10 stages with a top-brine temperature of 68.1 ºC and the highest value is for 6 stages with a top-brine temperature of 92 ºC. For low number-of-stages, the temperature difference is higher and the top-brine temperature in the first stage is lower. This is reflected in the heat transfer areas required for evaporation (**Fig. 6c)**. The heat transfer areas for higher top-brine temperatures are smaller compared to that for low top-brine temperatures. The specific heat transfer areas at 100ºC heat source temperature are 42% and 39% of that required at 70ºC when the number of effects are 6 and 10. These ratios resemble the observations reported by El-Dessouky et al [23]. This suggests that high temperature operation of MED results in lower heat transfer areas, and lower capital costs, however, at the expense of higher energy costs for the heat source.

4.4.2. Effect of Top Brine Temperature and Performance Ratio

The performance ratio (PR) of MED is defined as the kg of distillate produced by 2,300 KJ of heat input [25]. **Fig. 6d** establishes the relationship between the PR and the number of stages. In general, the PR decreases with increasing top-brine temperature. For example, when the number of stages (n) is 10, the PR is 9.6 and 9.8 while the top-brine temperatures were 95.5 ºC and 68.1 ºC. Similarly, for n = 6-9, the PR varies between 5.8-5.9; 6.7-6.9; 7.7-7.8; and 8.7-8.8 for heat source temperatures between 70 ºC and 100 ºC, high end PR representing low temperature operation. However, it can be noted that this difference is minimal and will not adversely affect the performance of the desalination plant [26].

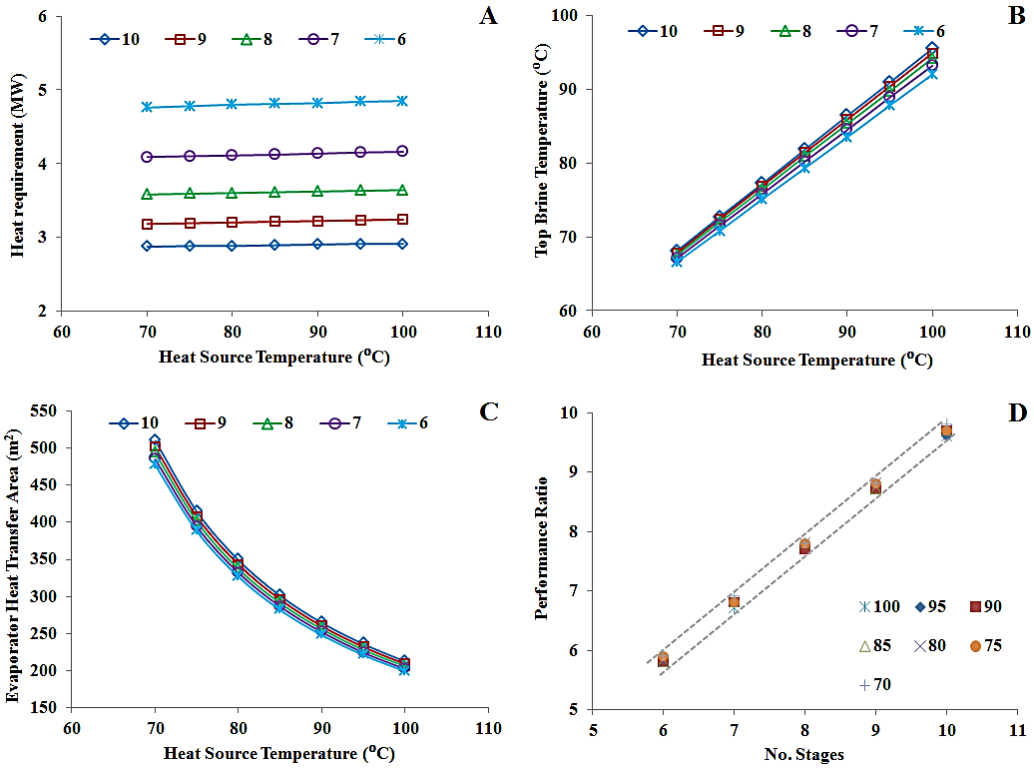

Figure 6. a) Heat requirements vs. source temperature; b) top brine temperature vs. source temperature; c) evaporator heat transfer area vs. source temperature; d) Performance ratio vs. number of stages

4.4.3. Number of Stages vs. Condenser Heat Transfer Area

Fig. 7a shows the relationship between the cooling water flow rate (kg/s) and the number of stages (n). The requirements for cooling water decreases with increasing values of 'n'. This is due to lower evaporating temperatures in the final condenser with higher values of 'n'. **Fig. 7a** shows the cooling water requirements (kg/s) as a function of available temperature differential (ΔT), i.e., 2.5-10 ºC. The cooling water requirements correspond to the return cooling water temperatures. Assuming the cooling water inlet temperature to be 5ºC, the flow rate increases when ΔT ranges from 2.5 to 10ºC (**Fig. 7a)**. At higher values of ΔT, the cooling water flow rates are significantly lower and vice versa. **Fig. 7b** shows the condenser heat transfer areas required for 'n' ranging from 6 to 10. Again, with the availability of temperature differential between the cooling water stream and condenser, the heat transfer areas changes with varying values of 'n'. The higher the ΔT, the smaller the condenser heat transfer area and vice versa. **Fig. 7c** shows the relationship between the brine temperatures in the last effect and the cooling water flow rates (kg/s). As expected, lower the value of 'n', higher the evaporating temperatures in the last effect, and higher the cooling water flow rates. As shown in **Fig. 7c**, they change with the available temperature differentials. Cooling water temperature differentials between 2.5 and 10 ºC are required to extract the latent heat from the final stage condenser with temperatures between 28 and 36 º C. Since TES unit chilled water temperatures vary between 5 and 20 ºC, a constant cooling water stream can be provided for all final condenser temperatures. **Fig. 7d** shows the brine outlet temperatures for different values of 'n'. Lower number of effects results in higher brine discharge temperatures, which in practice, are exchanged with the incoming seawater or feed water. This can be an issue in the Gulf and Mediterranean coastal areas since the incoming seawater temperatures can be as high as 35 ºC. Cooling water stream from TES enables MED operation with lower final condenser temperatures and lower brine discharge temperatures.

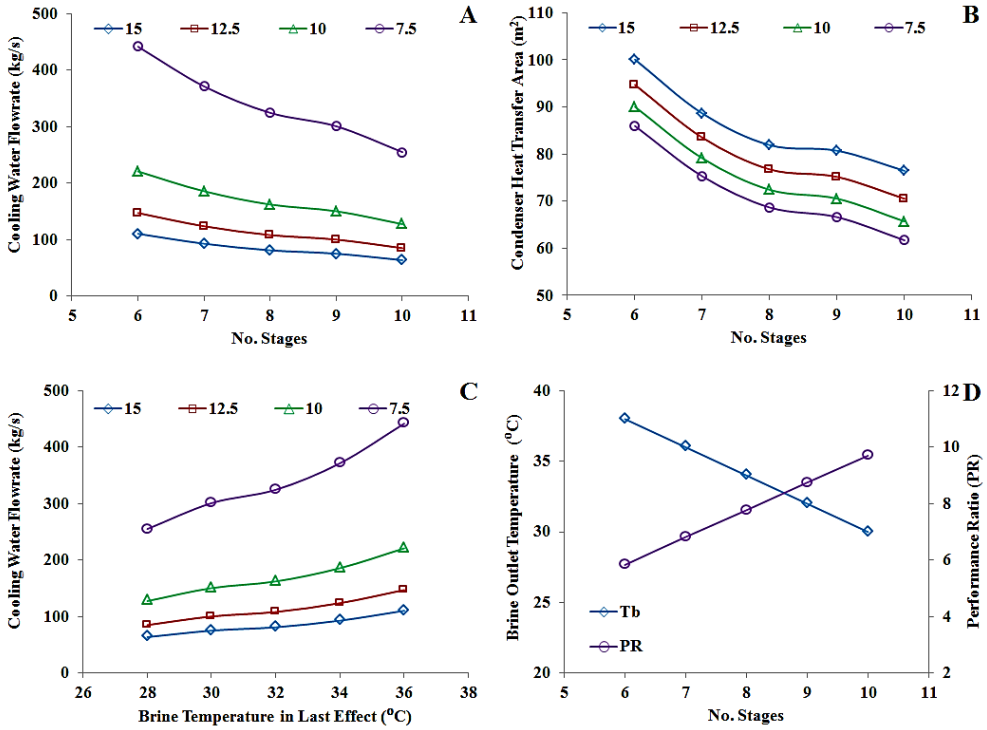

Figure 7. a) Cooling water flow rates vs. number of stages; b) condenser heat transfer area vs. number of stages; c) cooling water flow rates vs. brine temperature in last effect; d) brine outlet temperature vs. number of stages

CONCLUSIONS

We evaluated the feasibility of using waste heat to drive the absorption refrigeration system (ARS) and multi-effect evaporation desalination system in power plants. The ARS configuration was found to be effective in maintaining the temperature of chilled water in thermal energy storage (TES) which catered the cooling requirements in both MED and air-cooled condensers (ACCs). The TES system configuration was able to mitigate the disadvantages associated with use of ACCs in combined cycle power plants, especially during hot summers in arid regions of Nevada. The availability of waste heat from stack gas determines the sizing of ARS which in turn influences the size of storage tank. Availability of waste heat is a function of specific power plant configuration. The sizing and feasibility of MED system is again dependent upon the quantity and quality of brackish waters present at the site of a given power plant. The outcomes from this study provide a strong impetus to develop TES-based ACCs in power plants to reap the benefits of enhanced power production and low energy desalination system.

APPENDIX - MODELING STUDIES

Thermal Energy Storage (TES) System

The proposed TES meets the cooling requirements in i) air-cooled condensers (ACCs) of CCPP and ii) multi-effect evaporation desalination system (MED). The volume of the TES system can be estimated from a heat balance around the TES system described in the following equation:

$$V_s \rho_w C_{pw} \frac{d[T_s]}{dt} = -\dot{Q}_{.evap} + \dot{V}_a C_{pa} \rho_a (T_{amb} - T^*) + \dot{V}_{fc} C_{pw} \rho_w (T_{cw} - T_s) + K(T_{amb} - T_s) \quad (1)$$

Where $\dot{Q}_{evap}$ =heat required by the evaporator of ARS (kW); T_s = TES temperature in ºC; T_{cw} = temperature of cooling water from the final condenser (in desalination) in ºC. Other notations for the variables in **Eq 1** are described in nomenclature.

$\dot{V}_w > 0$ only if $T_{amb} > T^*$, otherwise $\dot{V}_w = 0$.

The first term on the right hand side of the **Eq 1** represents the heat removed by the ARS; second term is a heat input to TES, the heat removed from the inlet air to ACC; third term is another heat input to the TES, the heat rejected by the condenser in multi-effect desalination (MED). The last term in **Eq 1** represents the heat gained from the surroundings. The ambient temperature (T_{amb}) is a time-dependent that is largely influenced by the local meteorological conditions.

Analysis of CCPP

The operating details of a 500 MW CCPP were described in our earlier publication [1]. The rate of heat input to CCPP is 1,023 MW. The net output of the gas turbine is 320.1 MW while the steam turbine is rated at 170.9 MW. The rate of heat rejected by the condenser is 316.4 MW. The waste heat in the stack gases is available at a rate of 82.6 MW, and 86% of the waste heat is extracted from the stack gases (= 71 MW), out of which 66 MW is transferred to the generator of the ARS and another 4.96 MW is used in MED desalination. The standard design procedures were used to rate individual components of combined cycle power plants (**Eq**. 2-22).

Design Equations for Combined Cycle Power Plants

$$w_{g\_comp} = h_9 - h_8 \quad (2)$$

$$q_{in} = h_{10} - h_9 \quad (3)$$

$$w_{g\_turb} = h_{11} - h_{10} \quad (4)$$

$$w_{pump1} = h_2 - h_1 \quad (5)$$

$$w_{pump2} = h_4 - h_3 \quad (6)$$

$$w_{steam\_pumps} = (1-y) \times w_{pump1} + w_{pump2} \quad (7)$$

$$w_{steam\_turb} = h_5 - y \times h_6 - (1-y) \times h_7 \quad (8)$$

$$q_{out} = (1-y)(h_7 - h_1) \quad (9)$$

$$\dot{W}_{net} = \dot{m}_{gas} \times (w_{g\_turb} - w_{g\_comp}) + \dot{m}_{steam} \times (w_{steam\_turb} - w_{steam\_pumps}) \quad (10)$$

$$\eta_{th} = \frac{\dot{W}_{net}}{\dot{Q}_{in}} \quad (11)$$

$$\dot{W}_{net\_steam} = \dot{m}_{steam} \times (w_{steam\_turb} - w_{steam\_pumps}) \quad (12)$$

$$\dot{W}_{net\_gas} = \dot{m}_{gas} \times (w_{g\_turb} - w_{g\_comp}) \quad (13)$$

$$\dot{Q}_{gen} = 0.86 \times \dot{m}_{gas} \times (h_{12} - h_{13}) \quad (14)$$

3.3.1.2 Design Equations for Absorption Refrigeration System

$$\dot{Q}_c = \dot{m}_{2'} \times (h_{2'} - h_{4'}) \quad (15)$$

$$\dot{Q}_a = (h_{5'} \times \dot{m}_{5'}) + (h_{9'} \times \dot{m}_{9'}) - (h_{1'} \times \dot{m}_{1'}) \quad (16)$$

$$\dot{Q}_{gen} = (h_{2'} \times \dot{m}_{2'}) + (h_{3'} \times \dot{m}_{3'}) - (h_{6'} \times \dot{m}_{6'}) \quad (17)$$

$$\dot{Q}_{evap} = \dot{m}_{2'} \times (h_{5'} - h_{4'}) \quad (18)$$

$$P_{work} = \dot{m}_{1'} \times v_{1'} \times (HP - LP) \quad (19)$$

$$\eta_{hx} = (T_{3'} - T_{8'})/(T_{3'} - T_{7'}) \quad (20)$$

$$\dot{Q}_{hx} = \dot{m}_{3'} \times (h_{3'} - h_{8'}) \quad (21)$$

$$COP = \frac{\dot{Q}_{evap}}{\dot{Q}_{gen}} \quad (22)$$

Design Equations for Air Cooled Condensers

$$\dot{Q}_{out} = \dot{V}_a \times C_{pa} \times \rho_a \times (T^* - T_{out}) \quad (23)$$

3.3.2. Analysis of Multi-effect desalination system (MED)

The multi-effect evaporation was simulated with heat source temperatures ranging from 70 ºC to 100 ºC. The heat source is available at temperatures (steam from stack gases) suitable for the operation of a high temperature MED at a rate of 5 MW. We have studied the MED configuration by evaluating the effect of heat source temperature on the heat transfer areas, condenser areas, and the desalination capacity. Towards this end, the heating and cooling requirements were estimated under a range of brine temperatures and for different number of stages. Temperature differentials ranging from 2.5 ºC to 10 ºC were used to estimate the cooling water flow rate requirements for MED operation, at different number of stages and evaporation temperatures. The desalination capacity for a fixed amount of energy extracted from the stack gases was evaluated at low and high temperature (70 ºC to 100 ºC) operation of MED system. The design calculations were performed using **Eq.** 24-37 [24].

Temperature drop across all effects is obtained from the following relation:

$$\Delta T_t = T_s - (n-1)\Delta T_l - T_{b_n} \quad (24)$$

Temperature drop in first effect is obtained by

$$\Delta T_1 = \frac{\Delta T_t}{U_1 \sum_{i=1}^{n} \frac{1}{U_i}} \quad (25)$$

Similarly, the temperature drop in effects 2-n is obtained by

$$\Delta T_i = \Delta T_1 \frac{U_1}{U_i} \quad (26)$$

Brine temperature in first effect is obtained from the relation

$$T_{b_1} = T_s - \Delta T_1 \quad (27)$$

Brine temperature in effects 2 to n:

$$T_{b_i} = T_{b_i-1} - \Delta T_1 \frac{U_1}{U_i} - \Delta T_l \quad (28)$$

Distillate flow rate in the first is given by:

$$D_1 = \frac{M_d}{\lambda_{v_1}\left(\frac{1}{\lambda_{v_1}} + \frac{1}{\lambda_{v_2}} + ... + \frac{1}{\lambda_{v_{n-1}}} + \frac{1}{\lambda_{v_n}}\right)} \quad (29)$$

Distillate flow rate in effects 2 to n:

$$D_i = D_1 \frac{\lambda_{v_1}}{\lambda_{v_i}} \quad (30)$$

Brine flow rate in effects 1 to n

$$B_i = \frac{X_{cw} D_i}{(X_{bi} - X_{cw})} \quad (31)$$

Feed flow rate in effects 1 to n

$$F_i = D_i + B_i \quad (32)$$

Heat transfer area in the first effect

$$A_1 = \frac{D_1 \lambda_{v_1}}{U_1 (T_s - T_{b_1})} \quad (33)$$

Heat transfer area in effects 2 to n

$$A_i = \frac{D_i \lambda_{v_i}}{U_i (T_{v_i-1} - T_{b_i})} \quad (34)$$

Heat steam flow rate, M_s

$$M_s = \frac{D_1 \lambda_{v_1}}{\lambda_s} \quad (35)$$

Heat transfer area of the condenser

$$A_c = \frac{D_n \lambda_{v_n}}{U_c (LMTD)_c} \quad (36)$$

Flow rate of cooling water (M_{cw})

$$D_n \lambda_{v_n} = (M_{cw}) C_p (T_f - T_{cw}) \quad (37)$$

3.3.3. Analysis of TES

Eq 1 was solved numerically using the heat transfer value determined from the ARS analysis, T_{amb} obtained from hourly weather records, and cooling requirements from MED. **Eq 1** was solved by trial-and-error to obtain the optimal volume of the TES system, while ensuring that the TES temperature returned to its initial value at the end of each 365-day cycle. This analysis yielded the profiles of the TES temperature and the ACC inlet air temperature after pre-cooling. The value of T* was set at 20 ºC.

Nomenclature

Notations for CCPP, ARS, and TES

Symbols

ABS *Absorber;*
CC *Combustion chamber;*
COMP *Gas compressor;*
COND *Condenser;*
COP *Coeffecient of performance;*
CW *Chilled water;*
E, EVAP *Evaporator;*
G *Volumetric flow rate (m^3/s);*
GT *Gas turbine;*
GEN *Generator;*
HE *Heat exchanger;*
HP *High Pressure in ARS (kPa);*
h *Specific enthalpy (kJ/kg);*
K *Thermal conductivity, (W/m-K);*
LP *Low Pressure in ARS (kPa);*
m *Mass flow rate at point i (kg/s);*
OFWH *Open feed water heater;*
P *Pump;*
Q *Net heat transfer rate (MW);*
q *Specific net heat (kJ/kg);*
ST *Steam turbine;*
T *TES temperature,(ºC);*

T	Ambient temperature,(^oC);
T^*	Design temperature for Air inlet to ACC, (^oC)
t	Time (s);
V	Volume (m^3);
$\dot{V}$	Volumetric flow rate (m^3/s);
W^*	Power output (MW);
w	Specific net work (kJ/kg);
y	Mass fraction;
η	Efficiency;
ρ	Density (kg/ m^3);
v	Specific volume (m^3/kg);

Subscripts

a	absorber;
c	condenser;
e	evaporator;
g , gen	generator;
g_comp	gas compressor;
g_turb	gas turbine;
hx	heat exchanger;
in, i	inlet;
out	outlet;
s	storage;
$steam\_turb$	steam turbine;
th	thermal efficiency;
w	water;

Superscripts

$\bullet$ = indicates rate;

Notations for MED

A	Area, m^2
B	Brine flow rate from each evaporation effect, kg/s
Cp	Specific heat at constant pressure, kJ/kg EC
CR	Conversion ratio, CR = Md/Mf, dimensionless
D	Amount of vapor formed in each flashing stage or evaporation effect, kg/s
F	Feed flow rate to each evaporation effect, kg/s
$LMTD$	Logarithmic mean temperature difference
M	Mass flow rate, kg/s
n	Number of tubes, flashing stages, or evaporation effects
P	Pressure, kPa
PR	Performance ratio, PR = M_d / M_s, dimensionless
T	Temperature, ^oC
ΔT	Temperature drop, EC
ΔT_l	Temperature losses in each evaporation effect, ^oC
U	Overall heat transfer coefficient, kW/$m^2{}^oC$
V	Specific volume, m^3/kg
X	Salinity, ppm

Subscripts

λ	Latent heat for evaporation, kJ/kg
b	Brine
bh	Brine/feed preheater
c	Condenser or condensate
cw	Intake seawater
d	Distillate
e	Evaporator
f	Feed
h	Brine heater
j	Heat rejection section in MSF
o	Outer diameter or outlet temperature
n	Last flashing stage or last evaporation effect
r	Heat recovery section in MSF
v	Vapor

REFERENCES

1. Gadhamshetty V, Khandan NN, Myint M, and Ricketts C. Improving Air-Cooled Condenser Performance in Combined Cycle Power Plants, ASCE. Journal of Energy Engineering 2005;132(2): 81-88.
2. Conradie AE, Buys JD, and Kroger DG. Performance optimization of dry-cooling systems for power plants through SQP methods. Appl. Therm. Eng 1998; 18 (1–2): 25–45.
3. Al-Waked R and Behnia M. Performance evaluation of dry cooling systems for power plant applications. Appl. Therm. Eng 2004; 28: 147–161.
4. Owen MTF and Kröger DG. Numerical Investigation of Air-Cooled Steam Condenser Performance under Windy Conditions. California Energy Commission, PIER Energy-Related Environmental Research Program 2011. CEC-500-2011-021.
5. Maulbetsch JS and Di Filippo MN. Cost and Value of Water Use at Combined-Cycle Power Plants. California Energy Commission, PIER Energy-Related Environmental Research 2006. CEC-500-2006-034.
6. Gadhamshetty V and Khandan NN. Exergy analysis of Air-cooled Performance in Combined Cycle Power Plants. In CD-ROM proceedings of International Conference on Thermal Engineering and Application, Amman, Jordan, 2007.
7. Khandan NN, Gadhamshetty V, Mummaneni A. Improving Combined Cycle Power Plant Performance in Arid Regions. In CD-ROM proceedings of 6th International Conference on Heat Transfer, Fluid Mechanics and Thermodynamics, Pretoria, South Africa, 2008.
8. Szacsvay T, Posnansky M. Distillation desalination systems powered by waste heat from combined cycle power generation units. Desalination 2001;136: 133-140.

9. Wang Y, Lior N. Fuel allocation in a combined steam-injected gas turbine and thermal seawater desalination system. Desalination 2007; 214: 306–326.
10. Afgan NH, Darwish M, Garvalho G. Sustainability assessment of desalination plants for water production. Desalination 1999; 124:19–31.
11. Raluy RG, Serra L, Uche J, Valero A. Lifecycle assessment of desalination technologies integrated with energy production systems. Desalination 2004; 167: 445–458.
12. Mehmet AE, Aytunc E, and Dincer I. Energy and exergy analysis of an ice-on-coil thermal energy storage system, Energy 2011; 36: 6375-6386.
13. Gude VG, Khandan NN, Deng S. Sustainable low temperature desalination: A case for renewable energy. J. Renewable and Sustainable Energy 2011; 3 (043108):1-25.
14. Gude VG, Khandan NN, Deng S, Maganti A. Low temperature desalination using solar collectors augmented by thermal energy storage. Applied Energy 2012; 91: 466–474.
15. Hasnain SM, Alawaji SH, Ibrahim AA and Smiai MS. Applications of thermal energy storage in Saudi Arabia. International Journal of Energy Research 1999; 23(1): 119-120.
16. Yumrutas R and Kaska O. Experimental investigation of thermal performance of a solar assisted heat pump system with an energy storage. Int. J. Energy Res 2004; 28: 163–175.
17. Saman WY, Bruno F, and Halawa E. Thermal performance of a PCM thermal storage system with varying wall temperature. Solar Energy 2005; 78 (2): 341-349.
18. Ezan MA, Çetin L, and Erek A. Ice thickness measurement method for thermal energy storage unit. Journal of Thermal Science and Technology 2011; , 31: 1-10.
19. Powell KM, Cole WJ, Ekarika UF, & Edgar TF. Optimal chiller loading in a district cooling system with thermal energy storage. Energy 2013; 50: 445-453.
20. Verda V, Colella F. Primary energy savings through thermal storage in district heating networks. Energy 2011; 36(7): 4278-4286.
21. Fernandes D, Pitié F, Cáceres G, Baeyens J. Thermal energy storage: How previous findings determine current research priorities. Energy 2012; 39(1): 246-257.
22. A1-Shammiri M, Safar M. Multi-effect distillation plants: state of the art. Desalination 1999;126: 45-59.
23. El-Dessouky H, Alatiqi I, Bingula S, Ettouney H. Steady-State Analysis of the Multiple Effect Evaporation Desalination. Process Chem. Eng. Technol. 1998; 21:5439-451.
24. Al-Sahali M, Ettouney H. Developments in thermal desalination processes: Design, energy, and costing aspects. Desalination 2007; 214:227-240.
25. Aly NH, El-Fiqi AK. Thermal performance of seawater desalination systems. Desalination 2003;158:127-142.
26. Milow B, and Zarza E. Advanced MED solar desalination plants. Configurations, costs, future - seven years of experience at the Plataforma Solar de Almeria (Spain). Desalination 1996;108:51-58.